# Experimental Study on Gas Exploitation Performance Evolution of Fractured Hydrate-Bearing Sediments Under Shear

Shi Shen[2,*], Rui Qin[1,3], Haihong Chen[1,3], Ting Huang[1,3], Yang Ge[1,3], Xin Lv[2], Huiyong Liang[2]

[1]State Key Laboratory of Offshore Natural Gas Hydrates, Beijing, 100028, China
[2]Ningbo Institute of Dalian University of Technology, Ningbo, 315016, China
[3]China National Offshore Oil Corporation Research Institute Co. LTD, Beijing, 100028, China

*Corresponding Author: Shi Shen, shenshi_nbi@dlut.edu.cn

**Abstract.**Gas permeability of gas hydrate sediment is decisive factor that determines the rate of gas production during hydrate exploitation process. In site exploration indicates that hydrates are abundantly present in fractures of the reservoir, and the fractures provide convenient conditions for migration of fluids during the hydrate exploitation process. In this study, gas permeability evolution during triaxial shear process of fractured hydrate-bearing sediments was measured. The experimental results show that gas permeability damage of fractured hydrate-bearing sediment is affected by effective confining pressure. And as axial strain increases during shearing, gas permeability of fractured hydrate-bearing sediment generally presents a pattern of first decreasing, then increasing, and then decreasing again due to changes in fracture structure. And with increase of hydrate saturation, initial gas permeability, the peak permeability at rise and the minimum permeability at decline all increase. The conclusion of this study provides a data base for prediction of hydrate recovery efficiency of fractured hydrate sediments.

**Keywords:** Natural gas hydrate; Exploitation performance; Permeability; Triaxial shear process

## 1 Introduction

Natural gas hydrate (NGH) is a non-stoichiometric solid crystalline compound. Under standard conditions, the decomposition of 1 $m^3$ of NGH can release about 164 $m^3$ of natural gas [1], which is a kind of clean energy with abundant reserves and high efficiency [2]. In process of NGH exploitation, reservoir permeability is the key factor to determine gas production efficiency [3].

Reservoir deformation is associated with the exploitation of NGH by depressurization, heat injection or carbon dioxide replacement [4]. The deformation of reservoir affects the evolution of permeability during exploitation [5]. In addition, according to


W. He et al. (eds.), *Proceedings of the 2024 10th International Conference on Advances in Energy Resources and Environment Engineering (ICAESEE 2024)*, Atlantis Highlights in Engineering 36,
https://doi.org/10.2991/978-94-6463-708-3_6

the report of NGH exploration teams of China, the United States, India, Canada and South Korea, there are two main types of NGH occurrence: pore filling and fracture filling [6]. Fracture filled NGH mainly occurs in the fracture surface of siltstone, mudstone and oil shale [7]. Fractures provide convenient conditions for formation and accumulation of NGHs, and NGH accumulates in the form of veins, layers, nodules or blocks, which can be clearly observed from the pressure core [8]. They are an important part of reservoir matrix containing NGH and are very high quality NGH resources. Permeability in fractured reservoirs is key parameter controlling migration ability of natural gas and water fluids [9]. Permeability controls the seepage of gas/water in sediments and directly affects the production efficiency of methane gas. In process of gas production, the fluid flow process and geomechanical properties will be influenced by each other. The decomposition of NGH will weaken the strength of fractured sediments, resulting in formation deformation and settlement [10]. In turn, the mechanical changes of fractured sediment will affect porosity and permeability of reservoir [11]. Therefore, understanding dynamic evolution law of permeability in NGH fractured sediments during shear process and exploring influence mechanism of NGH saturation and effective confining pressure (ECP) changes on permeability characteristics of fractured reservoirs are the prerequisite for safe and efficient exploitation of NGH in fractured reservoirs.

In this paper, the gas permeability damage caused by ECP to fractured methane hydrate bearing sediments (MHBS) was studied by using mixture of standard sand and montmorillonite as sediments. In addition, the triaxial permeability measurement system was used to investigate the evolution of gas permeability of sediments with different methane hydrate (MH) saturation during the shear process. This study is of great significance to the development of NGH fractured reservoir.

## 2 Experimental Arrangement

### 2.1 Experimental System

In this paper, a set of triaxial mechanics and seepage testing equipment for MH was established to measure gas permeability of MH fracture sediments under shear behavior. The material of the triaxial pressure chamber is 316l stainless steel, which can withstand ECP not less than 16MPa. The model of the triaxial system is LF 50kN, its maximum range of load is 50kN, and the error is less than 0.05kN. The maximum stroke of axial load is 100mm, and its error is less than 0.125mm. The pressure chamber of the hydrate triaxial experimental system consists of two chambers: the inner chamber acts as a confining chamber, in which the sediment and silicone oil can be contained, and a 1mm rubber film was placed over the sediment to isolate it from the silicone oil. The outer chamber of the confining chamber is used for coolant circulation to provide a constant temperature for the sediments. The model of the circulating water bath used to control the temperature in the experiment is TMS8035-R40, whose temperature control range is -20~50°C, and the temperature error is 0.1°C. The sediment is located between the upper and lower pressure heads and is equipped with pores and inlet end was connected to the ISCO pump. The ISCO pump is a 260D with a volume capacity of

266.05ml. It is connected to the bottom of pressure chamber and provides pore pressure for the specimen, and the pressure error is 0.5% of the full range. During the experiment, permeable rock, sieve and filter paper were placed between the specimen and head hole, so as to prevent the sand from flushing into the pipeline during the seepage process. The permeability measurement acquisition relies on the differential pressure sensor (range 0 to 500kPa, error 0.16kPa), the back pressure valve (range 0 to 14MPa), and the flow sensor (error 0.001ml/min). In addition, the pressure and temperature in the experiment are collected by the related sensors and integrated in the module, and they are connected to the computer for recording. The schematic diagram of the above experimental setup is shown in Figure 1.

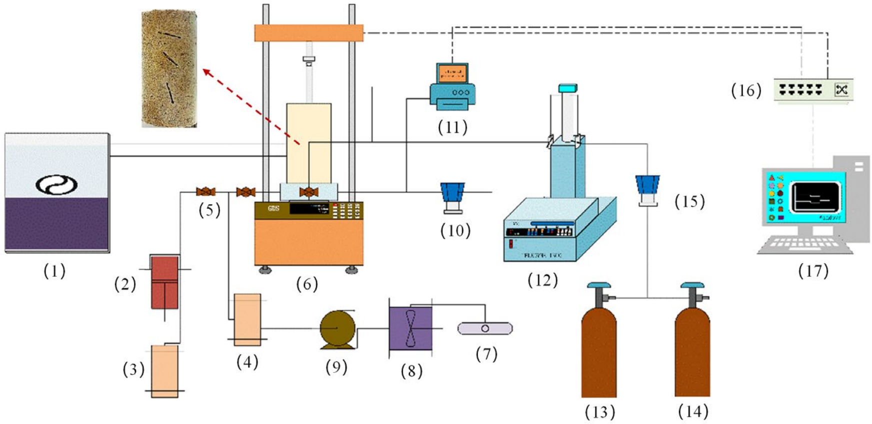


**Fig. 1.** Schematic diagram of experimental apparatus for hydrate triaxial permeability measurement

(1)Waterbath;(2)oil drum a;(3)oil drum b;(4)Oil pump;(5)Valve;(6)Triaxial;(7)Pressure controller;(8)Air compressor;(9)Gas-liquid booster pump;(10)Back pressure valve b;(11)Differential pressure transducer;(12)ISCO pump;(13)Nitrogen;(14)Methane gas;(15)Back pressure valve a;(16)AD modole;(17)Computer

## 2.2 Experimental Procedures

### 2.2.1 Specimen Preparation.

In this experiment, sand and montmorillonite were thoroughly mixed and stirred to prepare silty clay specimens with fractures of 50mm in diameter and 100mm in height. According to the designed water content, porosity and specimen size, the mass of the required soil specimen and volume of distilled water are calculated and weighed. In order to obtain the sediment with a porosity of 30%, it is calculated that the required materials for specimen preparation are 340g sand particles (95%) and 18g montmorillonite particles (5%). After the exact mass is weighed on the scale, they are poured into a sealed bag for thorough mixing, and then 27.4ml of distilled water is poured into the sealed bag with a measuring cylinder (the initial water saturation of the sediment is 40%). Water and soil specimens are carefully mixed to evenly distribute the water and obtain the final material mixture required for specimen preparation.

The mixed sand-montmorillonite mixture is equally divided into 10 parts, and then the triaxial specimen is prepared by filling it into the grinding tool specially made for the specimen through the funnel. First adjust the container with each portion of the mixture so that the material is evenly spread in the utensil. Then the gravity hammer is used to hit the molding (the beginning and the end are hit five times each, and the middle process is hit four times). Finally, the completed specimen is put into a professional fracture mold and drawn with diamond wire to make three fractures with a tilt Angle of 15°, 45° and 75°, with a length of 20mm and a width of 2mm. After the specimen is successfully made, seal it with plastic wrap and put it in the refrigerator. Let it stand for 24 hours to evenly distribute the water before taking it out and using it.

### 2.2.2 EXPERIMENTAL SCHEME.

In order to study the effect of shear on gas permeability of MHBS with different MH saturation, the constant pressure method was used to generate MH at 5MPa and 1°C. After a few hours, methane gas consumption on ISCO pump display showed little change, indicating that MH formation in sediment was complete. After MH formation, the sediments were consolidated with ECPs of 0.5 MPa, 1.0 MPa and 1.5 MPa. After the consolidation is completed, sediment was shear by triaxial method, and the permeability of the sediment is measured during the process of triaxial consolidation and shear. The pressure difference of the reaction chamber was recorded and effective gas permeability was calculated using Darcy equation (1). Table 1 shows the experimental conditions.

$$K_g = \frac{2QL\mu p_C}{A({P_1}^2 - {P_2}^2)} \tag{1}$$

Where, $K_g$ ($\mu$m$^2$) is measured permeability of HBCSs, $Q$ (ml/s) is fluids flow rate, $L$ (cm) is specimen length, $\mu$ (mPa • s) is fluids viscosity, $A$ (cm$^2$) is basal area of specimen, $P_1$ and $P_2$ are absolute pressure of inlet and outlet of system.

**Table 1.** Experimental conditions

| experimental conditions | (1) | (2) | (3) |
|---|---|---|---|
| MH sateration(%) | 0 | 20 | 40 |
| ECP(MPa) | 0.5 | 1.0 | 1.5 |
| Porosity | 0.3 | 0.3 | 0.3 |

# 3 Results and Discussions

## 3.1 Gas permeability Under Different ECPs

The effect of ECP on permeability was better understood and quantitatively analyzed, and the gas permeability failure rate was introduced. The penetration failure rate is defined as [12],

$$D_k = \frac{K_i - K_c}{K_i} \tag{2}$$

Where, $D_k$ is gas permeability failure rate under ECP, $K_i$ is initial permeability before ECP is applied, $K_c$ is permeability after ECP is applied.

When the MH saturation is 0% and the ECP is 0.5MPa, 1.0MPa and 1.5MPa, the initial permeability values of MHBS with fracture before consolidation are 0.04077 μm², 0.03558 μm² and 0.02985 μm², respectively. The consolidated permeability values of MHBS with fracture were 0.03686 μm², 0.0314 μm² and 0.02549 μm², respectively. When MH saturation is 40% and ECP is 0.5 MPa, 1.0 MPa and 1.5 MPa, the initial permeability values before consolidation of MHBS with fracture are 0.07079 μm², 0.05819 μm² and 0.068 μm², respectively. The consolidated permeability values of MHBS with fractures were 0.06279 μm², 0.05104 μm² and 0.058 μm², respectively.

According to equation (2), the corresponding permeability failure rate can be obtained, as shown in Figure 2. The results in the figure present that permeability damage rate increases with the increase of ECP. A reasonable explanation is that when the ECP is increased, the fractures and pores in the fractured sediment are compressed, resulting in a narrowing of the channels providing gas flow. The clay particles crushed by the ECP enter the fractures and pores in sediment, which has a significant impact on blockage of the seepage channels, resulting in a further decrease in permeability.

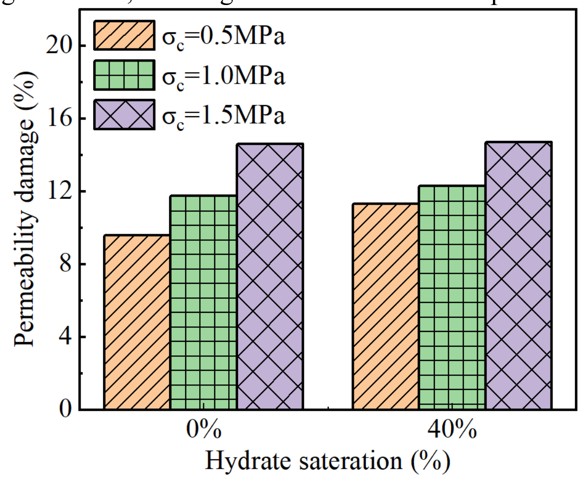


**Fig. 2.** Permeability damage rate of fractured MHBS

### 3.2 Gas Permeability Evolution of Fractured MHBS During Shear

Figure. 3 presents the permeability curves of fracture silty clay sediments with MH saturation of 0%, 20% and 40% under different ECPs. According to the data and the analysis of gas permeability curves in the three figures, it can be seen that with increase of axial strain, gas permeability of fractured sediments with MH saturation of 0 and 20% decreases first, then increases, and finally decreases gradually. The reason for the decrease is that the fractures and pores in the specimens are compressed and flow channels are narrowed. The reason for the increase is that with further increase of shear stress, failure surface is formed in interlayer contact position and MH fracture layer, and large-scale particle breakage occurs, and then a new flow channel is formed, and gas permeability increases accordingly. The second decline is due to the presence of many broken particles in the specimen at the initial shear stage, which fill the pores and fractures again. It not only blocked the fracture, but also blocked the reservoir around the fracture. The seepage channel is blocked again, resulting in a decrease in permeability. However, when the MH saturation is 40%, the permeability of the specimen decreases first and then increases with increase of axial strain, but the last decreasing trend does not appear. The reason for this result is that the enhanced permeability effect of gas seepage channels provided by cage MH and the weakened permeability effect of compression fractures and pores with the increase of ECP offset each other, resulting in a longer time for the permeability to decline and a longer time for the decrease to minimum permeability value, and the time for gas permeability to rise.

And with increase of MH saturation, initial gas permeability, the peak value of permeability during the rise and the lowest value of gas permeability during the fall of MHBS with fracture all show an increasing trend. There are two possible reasons for this behavior: First, when the pressure induced MH synthesis begins, the MH preferentially forms at gas-water interface. Because the gas-water interface in the fracture is more extensive than that in the surrounding particle pores, MH of large particles first appears along the inner surface of the fracture in the sediment in a short time, and some MH crystals appear in the form of pore filling in the single pore connected to the fracture. In the process of MH formation, water in pores and fractures will combine with methane gas to form a cage structure, and some new pores will be formed in the specimens containing fractures. Second, due to the good connectivity between fracture and surrounding pores, the whole MH in the region around the fracture is interconnected. Therefore, the agglomeration formed by the silty clay particles due to the charge interaction will not only enlarge the pores in the silty clay specimens with fractures, but also enlarge the fracture structure. However, the MH cannot completely fill the newly formed pores and enlarged fractures, thus providing a good seepage channel and increasing gas permeability.

In addition, it can be observed from Figure. 3 that with the increase of ECP, the initial permeability, the peak permeability during the rising process and the lowest permeability during the falling process of the silty clay specimen with fracture all show a decreasing trend. The reason is that ECP compresses the fractures and pores in the silty clay specimens with fractures, which reduces the channel for gas flow and leads to the decrease of gas permeability.

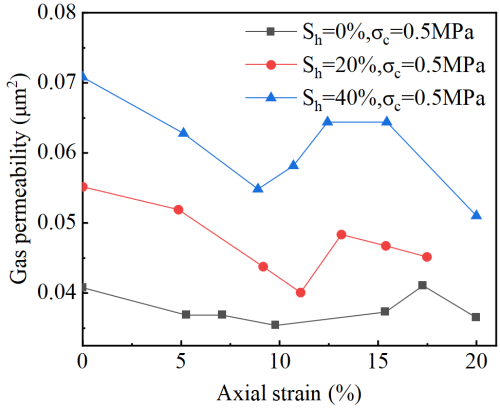


(A)

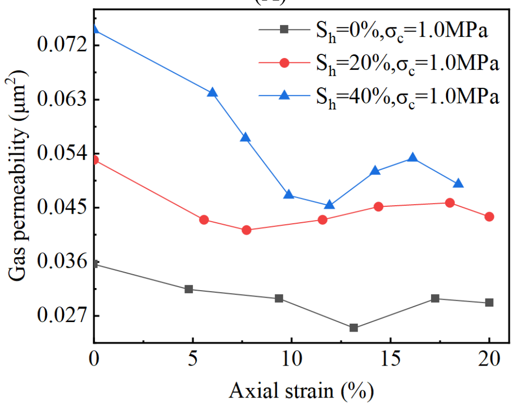


(B)

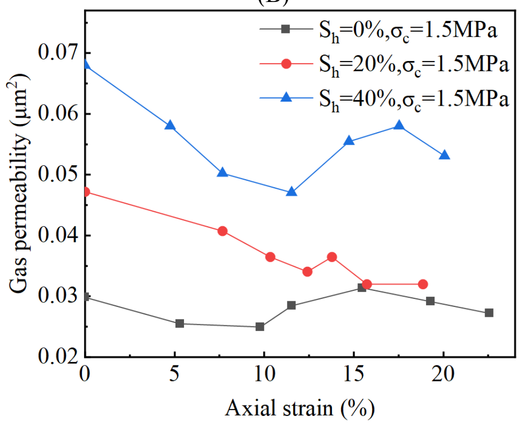


(C)

**Fig. 3.** Gas permeability variation of fractured MHBS with axial strain

# 4 Conclusion

In this study, the effect of ECP on gas permeability damage and the effect of shear process under the same ECP and MH saturation on gas permeability of fractured MHBS are analyzed respectively. The specific important conclusions are described below:

1. The permeability damage rate increases with the increase of the ECP.

2. With the increase of axial strain, the gas permeability of fracture sediments with MH saturation of 0 and 20% decreases first, then increases, and finally decreases gradually. When the MH saturation is 40%, gas permeability of specimen decreases first and then increases with increase of axial strain, but the last decreasing trend does not appear.

3. Due to the interaction between MH and clay particles, with increase of MH saturation, initial gas permeability, the peak permeability during the rise and the minimum permeability during the fall all show an increasing trend.

## Acknowledgements

This study was supported by the State Key Laboratory of Offshore Natural Gas Hydrates (2022-KFJJ-SHW), the Natural Science Foundation of Ningbo (2022J005).

## References

1. Wu, Z., Gu, Q., Wang, L., Li, G., Shi, C., He, Y., Li, Q., Li, Y., Experimental study on permeability and gas production characteristics of montmorillonite hydrate sediments considering the effective stress and gas slippage effect. SPE Journal, 2024. 29(5): p. 2525-2544.
2. Li, Y., Wei, Z., Wang, H., Wu, P., Zhang, S., You, Z., Liu, T., Huang, L., Song Y., Impact of hydrate spatial heterogeneity on gas permeability in hydrate-bearing sediments. Energy, 2024. 293: p. 130717.
3. Wang, H., Li, Y., Huang, L., Liu, T., Liu, W., Wu, P., Song, Y., A pore-scale study on microstructure and permeability evolution of hydrate-bearing sediment during dissociation by depressurization. Fuel, 2024. 358: p. 130124.
4. Wang, H., Liu, W., Wu, P., Pan, X., You, Z., Lu, J., Li, Y., Gas recovery from marine hydrate reservoir: Experimental investigation on gas flow patterns considering pressure effect. Energy, 2023. 275: p. 127482.
5. Wu, P., Chen, Y., Shang, A., Ding, J., Wei, J., Liu, W., Li, Y., Anisotropy analysis of two-phase flow permeability in the multi-stage shear process of hydrate-bearing sediments. Energy, 2024. 293: p. 130697.
6. Holland, M., Schultheiss, P., Roberts, J., Druce., M., Observed gas hydrate morphologies in marine sediments. International Conference on Gas Hydrates, 2008.
7. Sha, Z., Liang, J., Zhang, G., Yang, S., Lu, J., Zhang, Z., McConnell, D.R., Humphrey, G., A seepage gas hydrate system in northern South China Sea: Seismic and well log interpretations. Marine Geology, 2015. 366: p. 69-78.
8. Meng, Q., Liu, C., Lu, Z., Hao, X., Li, C., Bu, Q., Ji, Y., Wang, J., Growth behavior and resource potential evaluation of gas hydrate in core fractures in Qilian Mountain permafrost area, Qinghai-Tibet Plateau. China Geology, 2023. 6(2): p. 208-215.

9. Gong, G., Zhao, G., Pang, W., Yang, M., Chen, B., Zheng, J., Review of hydrate-bearing sediment permeability for natural gas hydrate exploitation: Measurement and application development. Journal of Petroleum Science and Engineering, 2023. 220: p. 111217.
10. Wan, Y., Wu, N., Hu, G., Xin, X., Jin, G., Liu, C., Chen, Q., Reservoir stability in the process of natural gas hydrate production by depressurization in the Shenhu area of the South China Sea. Natural Gas Industry B, 2018. 5(6): p. 631-643.
11. Zhu, C., Jiao, X., Cheng, S., Li, Q., Liu, K., Shan, H., Li, C., Jia, Y., Visualising fluid migration due to hydrate dissociation: implications for submarine slides. Environmental Geotechnics, 2020. 10(3): p. 218-226.
12. Wang, H., Liu, W., Sun, X., Pan, X., Li, Y., Experimental study on the gas permeability of marine sediments with various hydrate saturations and effective stresses. Energy Fuels, 2021. 35(21): p. 17479-17489.